Hou, Yifan, Wang, Shihui, Ma, Yukun, Shen, Zhenyao, & Goonetilleke, Ashantha
(2023)
Influence of landscape patterns on nitrate and particulate organic nitrogen inputs to urban stormwater runoff.
Journal of Environmental Management, *348*, Article number: 119190.

https://doi.org/10.1016/j.jenvman.2023.119190

Influence of landscape patterns on nitrate and particulate organic nitrogen inputs to urban stormwater runoff

Yifan Hou[a], Shihui Wang[a], Yukun Ma[a,*], Zhenyao Shen[a], Ashantha Goonetilleke[b]

[a] State Key Laboratory of Water Environment Simulation, School of Environment, Beijing Normal University, 19 Xinjiekou Outer Street, Beijing, 100875, PR China

[b] Science and Engineering Faculty, Queensland University of Technology (QUT), GPO Box 2434, Brisbane 4001, Queensland, Australia

*Corresponding author
Yukun Ma
Email: ykma@bnu.edu.cn

Influence of landscape patterns on nitrate and particulate organic nitrogen inputs to urban stormwater runoff

Abstract: This study investigated the effect of the landscape pattern of permeable/impermeable patches on NO_3^--N and particulate organic nitrogen (PON) concentrations during stormwater runoff transport and their source contributions. Six landscape pattern indices, namely, the mean proximity index (MPI), largest patch index (LPI), mean shape index (MSI), landscape shape index (LSI), connect index (CONNECT), and splitting index (SPLIT), were selected to reflect the fragmentation, complexity, and connectivity of permeable patches in urban catchments. The results show that lower fragmentation, higher complexity, and greater connectivity can reduce NO_3^--N concentrations in road runoff and drainage flow (i.e., the flow in the stormwater drainage network), as well as PON concentrations in road runoff. Low impact development (LID) can be incorporated with the landscape pattern of permeable/impermeable patches to mitigate nitrogen pollution in urban stormwater at the catchment scale by optimizing the spatial arrangement.

Keywords: permeable/impermeable patches; landscape pattern; low impact development; nitrate; particulate organic nitrogen; stormwater quality

1 Introduction

Stormwater runoff from urban areas is a major source of receiving water quality degradation. This is further exacerbated by the escalating urbanization witnessed in many parts of the world (Chen and Guo, 2022; Pamuru et al., 2022; Peter et al., 2022). Sources such as plant debris, animal litter, lawn fertilizer and vehicle exhaust emissions can result in significant amounts of nitrogen inputs to urban receiving waters which is a primary stormwater pollutant (Christensen et al., 2021; Huang et al., 2021; Xie et al., 2021). Excessive nitrogen inputs can lead to the deterioration of aquatic ecosystems (Ding et al., 2023; Meng et al., 2022). The two forms of nitrogen commonly found in urban stormwater are dissolved nitrogen such as nitrate (i.e., NO_3^--N) and particulate nitrogen such as particulate organic nitrogen (PON) (Jani et al., 2020). The excessive input of NO_3^--N and PON to water can lead to eutrophication, hypoxia, and loss of biodiversity (Balasuriya et al., 2022; McAleer et al., 2022; Priestley et al., 2022). Therefore, the protection of water ecosystem values requires the mitigation of NO_3^--N and PON pollution through the implementation of effective stormwater management strategies (Lucke et al., 2018; Pilon et al., 2019).

Urban catchments with a high proportion of permeable surfaces have been found to have relatively lower concentrations of nitrogen pollutants in stormwater runoff (Brown and Borst, 2015; Simpson et al., 2022; Wu et al., 1998). This is because permeable surfaces such as lawns and vegetated areas have a relatively higher ability to retain nitrogen pollution contained in urban stormwater runoff compared to impermeable surfaces (Ferreira et al., 2016; Teixeira and Marques, 2016a; Zhang et al., 2019a). It is in this context that Low Impact Development (LID) can play a role in stormwater pollution mitigation. LID is an urban stormwater management concept that emphasizes source-dispersed and small-scale control facilities to effectively mitigate increased flood flows, runoff coefficients and surface source pollution loads caused by the increase in impermeable area (Eckart et al., 2017; Pour et al., 2020; Xu et al., 2019). Urban areas provided with LID measures can essentially be considered as permeable surfaces which can effectively reduce nitrogen pollution in stormwater runoff (Duan et al., 2013; Kamali et al., 2017). Therefore, optimizing the spatial arrangement of LID within an urban catchment is important to mitigate the nitrogen load in stormwater runoff. This requires an in-depth understanding of the influence of LID layout on nitrogen transport at the catchment scale. Nitrogen contained in urban stormwater is mainly derived via three transport stages, namely, roof runoff, road runoff and stormwater drainage flow (i.e., the flow in the stormwater drainage network) (Ma et al., 2021; Wang et al., 2022). The transport of nitrogen is significantly influenced by the landscape pattern of permeable/impermeable patches, as permeable surfaces can intercept the runoff from impermeable surfaces. Furthermore, the variation in runoff transport can influence the input of nitrogen from each transport stage to urban stormwater discharged at the catchment outfall. In other words, the primary nitrogen inputs can be manipulated by changing the landscape patterns (Christensen et al., 2019; Hu et al., 2023; Wu et al., 2022). Therefore, understanding the influence of permeable/impermeable landscape patterns on nitrogen transport is important for mitigating nitrogen pollution by changing stormwater transport patterns and sources. The current paucity of knowledge in the context of landscape indices constitutes a significant knowledge gap in relation to the design and siting of LID to achieve effective stormwater treatment. Landscape indices are simple quantitative indicators that highly condense information about a landscape pattern to characterize some aspect of its structural composition and spatial configuration (Thangarajan et al., 2018; Valenca et al., 2021; Xia et al., 2020). Most previous studies have focused on the effects of LID technologies on stormwater quality and quantity at the end discharge point from a catchment (Ferreira et al., 2019; Jiang et al., 2020; Yao et al., 2021). However, there is a lack of knowledge about the influence of LID spatial configuration on pollution transport within a catchment. Optimizing the spatial configuration of LIDs in urban catchments to improve their ability to reduce runoff and pollutant concentrations has been a focus of interest of researchers (Sui and van de Ven, 2023; Tirpak et al., 2021). It can provide recommendations for the spatial arrangement of LIDs for runoff regulation and pollution mitigation. Therefore, it is important to further explore how the deployment of LIDs can be optimized to reduce stormwater pollution in urban catchments (Zhang et al., 2023).

The main objectives of this study were: (1) to analyze the effect of the landscape pattern of permeable/impermeable patches in the form of landscape indices on the transport and sources of NO_3^--N and PON in urban stormwater runoff; and (2) to provide recommendations for the spatial arrangement of stormwater management measures such as LID for nitrogen pollution mitigation. In this study, the correlation between the landscape pattern indices and pollutant concentrations and source contributions was evaluated to determine the influence of the landscape pattern on the transport and source of NO_3^--N and PON. Based on the above findings, recommendations are provided for the spatial arrangement of LIDs in urban catchments. The results of this study are expected to enhance the understanding of the role of landscape pattern of permeable/impermeable patches on nitrogen pollutants in urban stormwater at the catchment scale, as well as contribute new knowledge for the optimization of LID siting and design for the mitigation of stormwater nitrogen pollution.

2 Materials and methods

2.1 Sampling sites

Beijing City which is situated in the northern North China Plain has a warm-temperate semi-humid monsoon climate. It encompasses an area measuring 16,410 km^2. Two study areas were selected for this research project, namely, Beijing Normal University (BNU) in Haidian District, Beijing, and Future Science City (FSC) in Changping District, Beijing. These two study areas were selected due to the same geographic location and similar climate, drainage network and permeability. BNU (latitude 39°57 N and longitude 116°21 E) is located close to FSC (latitude 30°27 N and longitude 119°98 E). The two study areas have separate stormwater and wastewater drainage networks. Therefore, it was acceptable to compare the characteristics of the pollutants in the two stormwater conveyance systems. The permeability of the two study areas was derived using ArcGIS to assess the proportion of the permeable patch area to the total area. Their permeability rates are similar, i.e., 37% and 35% for BNU and FSC, respectively. BNU has 36% of grass and woodland, 1% of bare land, 28% of roads and 35% of roofs, while FSC has 12% of grass and woodland, 19% of bare land, 36% of roads, 25% of roofs and 7% of construction land. The most obvious difference between the two study areas is the landscape pattern of the permeable areas. BNU has a large area of grassland and woodland with good connectivity and a complex green landscape profile, whereas FSC has more dispersed grassland and woods, which are interspersed with large areas comprising roofs and roads. Figure 1 shows the characteristics of the two study areas. Although the hydrological, climatic and landscape characteristics of the two study areas selected were similar, it is important to note that the focus of the research study was to investigate the role of the landscape pattern of permeable/impermeable patches in influencing stormwater pollution. Therefore, the key novelty of this study was the explicit accounting of the role of the landscape pattern in terms of permeable/impermeable patches in dictating nitrogen pollution, which in turn would enable the adoption of effective spatial arrangement strategies of LIDs.

Accordingly, the key study outcomes are generic and would be equally applicable to other urban areas with different climate and hydrological conditions.

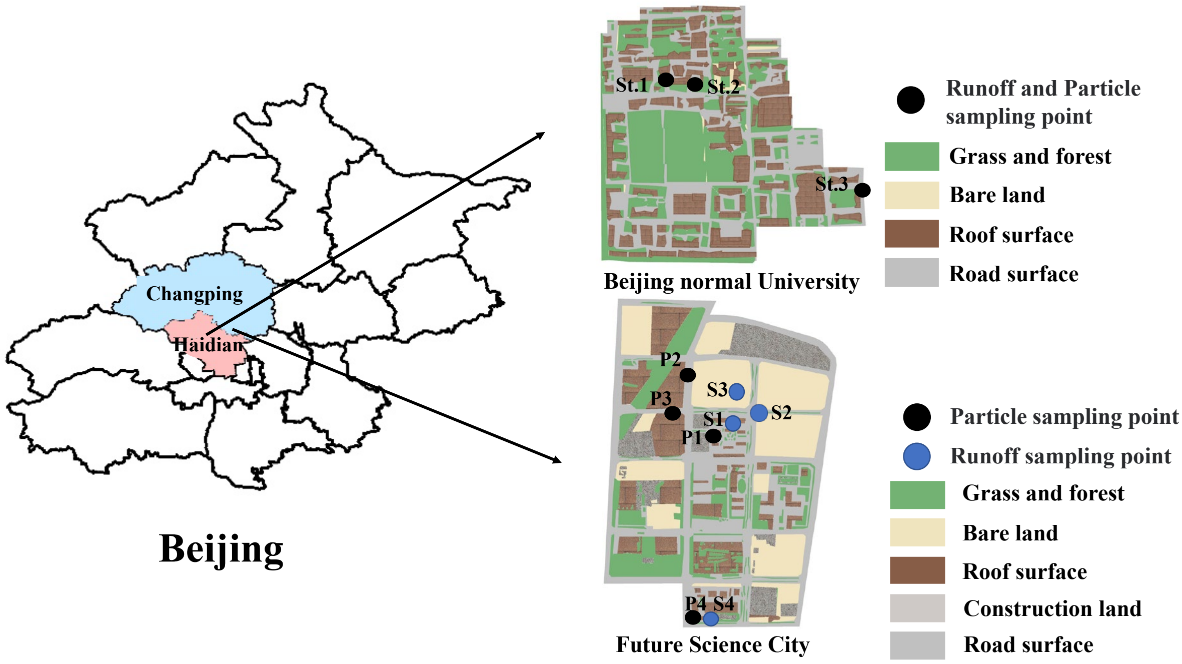

Figure 1. Study area and sampling sites.

BNU consists of five catchments, and the largest catchment was selected for this study. Sampling sites 1 (St.1) and 2 (St.2) were selected for collecting roof and road runoff, respectively. The drainage outlet in the study catchment was located at St.3, where the drainage flow delivered via subsurface stormwater pipes was collected (see Fig. 1). Since PON in stormwater discharged from the catchment was from build-up particulates washed-off by roof runoff, road runoff and drainage flow, roof and road deposited samples and drainage sediments during the dry periods were also collected. It was assumed that PON attached to build-up solids was consistent with PON attached to suspended solids in the runoff. Roof deposited sediments were collected from St.1, which was the same roof where roof runoff was collected. Road deposited sediments were collected from St.2. Drainage sediments were obtained from a drainage pipeline near St.3.

There are three catchments in FSC and the largest catchment was selected for this study. Four sampling sites (S1–S4) were selected to collect runoff samples and four sampling sites (P1–P4) were selected to collect particulate samples during the dry period. Roof runoff was collected at S1; road runoff was collected at S2, which was located on a road near S1; and rainwater was collected at S3, which was located on a vacant plot close to S1 and S2 (see Fig. 1). The drainage flow samples were collected from the end of the stormwater outflow (S4), which discharged directly to a waterway. Roof deposited sediments were collected at P1, which was located on the same roof where roof runoff was collected. Particulate samples on commercial and residential area road surfaces were collected at P2 and P3, respectively and drainage sediments were collected at P4, which was located in the stormwater drainage pit.

2.2 Sample collection

The roof, road, and drainage flow samples were collected using plastic beakers. Rainwater was collected using a polyethylene bottle during each rainfall event. To adequately reflect the first flush phenomenon (Deletic, 1998), the sampling intervals were set as 5 min for the first 15 min, 15 min for the next 15–60 min, and 30 min after 60 min. At BNU and FSC, 123 (45 road runoff samples, 39 roof runoff samples, and 39 drainage runoff samples) and 434 (149 road runoff samples, 144 roof runoff samples, 141 drainage runoff samples) runoff samples were collected during five and thirteen rainfall events, respectively. Each runoff sample was transferred to a labelled 500 mL glass bottle and stored at 4 °C until laboratory analysis. A vacuum cleaner (Philips FC9735) was used to collect particulate samples on roofs and roads from a 1 m × 2 m area. Particles build-up on roofs and roads during dry days can be washed-off with stormwater runoff. Since the physical and chemical properties of particles can change during the wash-off process, the dry particles were collected for more accurate source apportionment. Drainage sediments were obtained at 10 cm from the rainwater grate using a shovel. A total of 123 and 122 particulate samples from BNU and FSC, respectively, were fully ground, sieved through a 200-mesh sieve, and then stored in sealed plastic bags at 4 °C until analysis. Rainfall data were recorded using a rain gauge (TD-F3L), and the rainfall characteristics are listed in Table 1. Although samples were collected from different years in the two catchments, the rainfall characteristics such as rainfall types, rainfall amount and rainfall intensities were similar. All rainfall events monitored were during summer and autumn where the rainfall amount accounts for 85% of the annual rainfall in Beijing (Zhang et al., 2014). Therefore, it was hypothesized that it was acceptable to compare the data collected from the two catchments.

Table1. Characteristics of the monitored rainfall events.

Rainfall Event	Rainfall Date	Rainfall Depth (mm)	Rainfall Duration （h）	Average Rainfall Intensity (mm/h)	Antecedent Dry Period (days)	Catchment
Event 1f	2021/5/31	2.5	1.4	1.8	0.3	FSC
Event 2f	2021/6/9	8.8	4.3	2	0.8	FSC
Event 3f	2021/6/16	3.4	3.7	0.9	5.5	FSC
Event 4f	2021/6/25	17	5	3.4	1.6	FSC
Event 5f	2021/7/1	19.1	2.4	8	5.7	FSC
Event 6f	2021/7/3	50.1	5	10	1.3	FSC
Event 7f	2021/7/5	7.8	2.3	3.4	2.2	FSC
Event 8f	2021/7/11	32.4	1	32.4	3.2	FSC
Event 9f	2021/7/18	21.3	4.5	4.7	1.1	FSC
Event 10f	2021/7/29	4.8	5.3	0.9	1.7	FSC
Event 11f	2021/8/9	3.6	2.2	1.6	4.9	FSC
Event 12f	2021/8/15	30.5	2.4	12.7	0.6	FSC
Event 13f	2021/8/19	21.3	11.5	1.9	2.4	FSC
Event 1b	2019/7/5	5.8	13	0.8	2.7	BNU
Event 2b	2019/7/22	20.2	7	2.2	2.5	BNU
Event 3b	2019/8/4	36.4	56.5	2.8	2.4	BNU
Event 4b	2019/8/20	8.6	7.7	0.4	7.3	BNU
Event 5b	2019/10/4	24	8.5	2.6	20.9	BNU

2.3 Laboratory analysis

The concentrations of NO_3^--N and PON were determined for the roof and road runoff and drainage flow. The nitrate isotopes ($\delta^{15}N$-NO_3^- and $\delta^{18}O$-NO_3^-) were measured for the rainwater, roof runoff, road runoff and drainage samples, while the PON isotopes ($\delta^{13}C$-PON and $\delta^{15}N$-PON) in the collected particulate samples were also measured. Each sample was separated into three subsamples and measured separately and the mean values were used as the final values. Nitrogen concentrations were determined according to national standard protocols (PRCMEP, 2002). The runoff samples were categorized into two groups. One group was used to determine the total nitrogen (TN) and PON. The other group was filtered using a 0.45 μm microporous membrane. The filtrate was acidified with sulfuric acid to pH < 2, and the concentrations of total dissolved nitrogen (TDN) and NO_3^--N were determined within 24 h. A curve was constructed using the standard NO_3^--N solution as the horizontal axis and the absorbance in ultraviolet spectrophotometry (UV-6100) as the vertical axis. The concentration of NO_3^--N was determined using UV spectrophotometry (HJ 636-2012). The NO_3^--N concentration was quantified by measuring the absorbance of nitrate ions at 220 nm. Two sets of runoff samples were aliquoted and the concentrations of TN and TDN were determined separately. The TN and TDN in the two runoff samples were oxidized to NO_3^--N using $K_2S_2O_8$. The oxidized mixture was placed in a high-pressure steam tank and maintained at a temperature between 120 °C and 124 °C for 30 min. Before measuring the absorbance at 220 and 275 nm, 1 mL of hydrochloric acid was added to the mixture. The NO_3^--N concentration was determined based on the curve of the NO_3^--N concentration corresponding to the measured absorbance and the TN and TDN concentrations. The PON concentration can be expressed as [PON] = [TN] - [TDN]. The concentration of NO_3^--N was determined directly via UV spectrophotometry without digestion and heating. NO_3^--N and PON concentrations are the concentrations of nitrogen in stormwater runoff in nitrate and particulate forms, respectively. The mean concentration of NO_3^--N and PON for each rainfall event was expressed as event mean concentration (EMC). EMC is usually defined as the mass of the pollutant contained per unit of runoff volume during a unit rainfall event (Peng et al., 2016). It can be defined as a mathematical formula as follows (Perera et al., 2021):

$$EMC = \frac{\int_0^T C(t)Q(t)dt}{\int_0^T Q(t)dt}$$

where $C(t)$ and $Q(t)$ are time variable concentration and the flow rate, respectively. T is the event duration.

The isotopes of the nitrates ($\delta^{15}N$-NO_3^- and $\delta^{18}O$-NO_3^-) were analyzed using the bacterial denitrification method (McIlvin and Casciotti, 2011), and an isotope mass spectrometry (Isoprime100, Cheadle, UK) was undertaken to determine the isotopes.

The particulate samples were acidified with hydrochloric acid to remove inorganic compounds present, and an isotope mass spectrometer (Isoprime100, Cheadle, UK) was connected to an elemental analyzer to determine the PON isotopes ($\delta^{13}C$-PON and $\delta^{15}N$-PON). The ratio of stable isotopes can be expressed using the delta (δ) sign and per mil (‰) as follows:

$$\delta_{sample} = \left(\frac{R_{sample}}{R_{standard}} - 1\right) \times 1000$$

where R_{sample} and $R_{standard}$ represent the $^{15}N/^{14}N-NO_3^-$, $^{18}O/^{16}O-NO_3^-$, $^{13}C/^{12}C$-PON, and $^{15}N/^{14}N$-PON ratios of the samples and standards, respectively. The values of $\delta^{15}N$, $\delta^{18}O$, and $\delta^{13}C$ correlate with the values of atmospheric N_2, $\delta^{18}O$, and $\delta^{13}C$, respectively, based on the Vienna Standard Mean Ocean Water and Vienna Pee Dee Belemnite standards. Each sample was analyzed five times in isotopic analysis.

2.4 Statistical analysis

2.4.1 Landscape pattern analysis

Remote sensing data from the catchment area were visually interpreted using ArcGIS 10.7 to classify the land use of the catchment area based on permeable/impermeable patches. Bare land, woodland, and grass were classified as permeable patches, whereas roofs, roads, and construction land were classified as impermeable patches. The landscape pattern index is a simple quantitative index that can highly condense information about the landscape pattern and reflects certain aspects of the composition and spatial configuration of its structure (Wu et al., 2021). To calculate the patch class level landscape pattern indices, a map of classified permeable/impermeable patches can be input into the FRAGSTAT 4.2.1 software. The landscape pattern indices used are discussed in Section 3.1. The landscape pattern indices of permeable patches were used to describe the landscape patterns of permeable/impermeable surfaces in the catchments of interest.

2.4.2 Source apportionment calculation

The MixSIAR model was used to determine the primary NO_3^- contributing sources in drainage flow, roof runoff, road runoff, and rainwater, as well as the primary PON contributing sources in suspended solids in roof runoff (i.e., roof deposited sediments), suspended solids in road runoff (i.e., road deposited sediments) and suspended solids in drainage flow (i.e., drainage sediments). The model is expressed as follows (Parnell et al., 2013):

$$X_{ij} = \sum\nolimits_{k=1}^{k} p_k\left(S_{jk} + C_{jk}\right) + \varepsilon_{ij}$$

$$S_{jk} \sim N(U_{jk}, {\omega^2}_{jk})$$

$$C_{jk} \sim N(\lambda_{jk}, {\tau^2}_{jk})$$

$$\varepsilon_{jk} \sim N\left(0, {\sigma^2}_{jk}\right),$$

where X_{ij} is the isotopic value j of sample i (i = 1,2,3,...,N; j = 1,2,3,...,j); Pk is the proportion of source k (k = 1,2,3,...,k) estimated using the SIAR model; S_{jk} is the source value k of isotope j, which is normally distributed with λ_{jk} as the mean and $\tau^2{}_{jk}$ as the standard deviation; and ε_{jk} is the residual that represents the additional unquantified variation between samples.

2.4.3 Analysis of variance (ANOVA)

Statistical comparisons of spatial and temporal differences in NO_3^--N and PON concentrations and contributions of different transport stages were performed via ANOVA. Post-hoc comparisons of the mean NO_3^--N concentrations and contributions between the two catchments were conducted to determine the magnitude of the association. Values of $p > 0.05$ indicate no significant differences, whereas values of $0.01 < p < 0.05$ indicate significant differences. Values of $p < 0.01$ indicate highly significant differences.

2.4.4 Pearson correlation analysis

Pearson correlation analysis was performed to determine the relationship between landscape pattern indices and concentrations and source contributions. Pearson correlation analysis has been used extensively to analyze the correlation between landscape patterns and the water quality in catchments (Li et al., 2015a). Correlation coefficients are used to determine the degree of correlation: a correlation coefficient of 0.8 to 1.0 indicates a high correlation; 0.5 to 0.8, a moderate correlation; and 0.3 to 0.5, a low correlation. Pearson correlation analysis was performed using SPSS version 26.0. Each landscape pattern index was tested individually for all nitrogen indicators. The correlation coefficients ranged from -1 to 1 based on ‘analytically correlated bivariate-correlation’ analysis, with p values of 0.01 and 0.05 for permutation testing. The parameters were selected based on the number of correlated parameters.

3 Results

3.1 Comparison of landscape patterns at BNU and FSC

The differences in landscape characteristics between BNU and FSC are presented in Section 2.1. Previous studies found that the area ratio, circumference, shape and patch connectivity of permeable surfaces have the most significant influence on stormwater runoff pollution in urban catchments (Ma and Zhao, 2022a; Shen et al., 2014). In other words, landscape patterns that could characterize the permeability fragmentation, shape complexity and permeability convergence were considered in this study. Accordingly, six landscape pattern indices were selected to quantitatively describe the differences in landscape pattern between BNU and FSC: the mean proximity index (MPI), largest patch index (LPI), mean shape index (MSI), landscape shape index (LSI), connect index (CONNECT) and splitting index (SPLIT). MPI and LPI represent the extent of permeability fragmentation. MPI is the number of permeable patches per unit area. LPI refers to the percentage of the largest area of permeable parcels in the catchment relative to the total area. MSI and LSI represent permeability complexity. MSI represents the level of complexity of an individual permeable patch. LSI refers to the complexity of the permeable patch shapes. CONNECT and SPLIT represent the permeability convergence. CONNECT is the functional connectivity between permeable patches. SPLIT is the degree of separation of permeable patches in the catchment. Table 2 shows a comparison of the landscape pattern indices for BNU and FSC. The LPI and MPI of BNU were significantly higher than those of FSC, suggesting that permeable patches at BNU are less fragmented than at FSC. The LSI and MSI of BNU were higher than those of FSC, suggesting that permeable patches in BNU are more complex in shape compared to FSC. The CONNECT of BNU is higher than that of FSC, whereas the SPLIT is lower than that of FSC, suggesting that BNU has better permeable surface connectivity than FSC.

Table 2. Comparison of landscape pattern indices for BNU and FSC.

Landscape patterns	Fragmentation		Complexity		Convergence	
	MPI	LPI	LSI	MSI	CONNECT	SPLIT
BNU	76.4736	13.0792	14.8072	1.6104	5.8252	52.9074
FSC	32.9254	4.6566	8.9681	1.2522	1.9987	100.4824

3.2 Comparison of NO_3^--N and PON concentrations during stormwater transport

Figure 2 shows the mean concentrations of NO_3^--N and PON during stormwater transport from different rainfall events in the two catchments. As shown in Figure 2, the PON concentration in roof runoff from BNU (mean, 0.74 mg/L) was slightly less than that from FSC (mean, 0.87 mg/L). The PON concentration in road runoff from BNU (mean, 2.15 mg/L) was significantly lower than that from FSC (mean, 3.44 mg/L; ANOVA, $p < 0.05$). This is attributed to the fact that the roads at BNU are connected to relatively larger lawns and woods with the larger permeable surfaces acting as large PON retention areas. Besides, owing to the complex shapes of the permeable surfaces in BNU, PON transport originating from the surrounding road surfaces is impeded and suspended solids are retained by the permeable surfaces to a greater extent. Additionally, the more explicit aggregation pattern between the permeable patches in BNU enhances the exchange of material and energy, as well as retaining more PON. The PON concentration in the drainage flow from BNU (mean, 5.49 mg/L) was significantly higher than that from FSC (mean, 3.01 mg/L; ANOVA, $p < 0.05$). This is attributed to the fact that the permeable surface at BNU is dominated by woodland, whereas at FSC is dominated by grassland. Previous studies have shown that vegetation debris and grass clippings from lawns constitute 76% and 24% of the PON in stormwater runoff, respectively (Lusk et al., 2020). The concentration of PON in the drainage flow from

BNU was higher than that from FSC, which is consistent with previous findings. The trend in PON concentrations in the two catchments at each transport stage was analyzed. PON concentrations in BNU increased in the order of roof runoff (mean, 0.74 mg/L) < road runoff (mean, 2.15 mg/L) < drainage runoff (mean, 5.49 mg/L), and the highest PON concentration was found in the drainage runoff. Different from BNU, PON concentration in FSC showed an increasing trend from roof runoff (mean, 0.87 mg/L) to road runoff (mean, 3.44 mg/L) and then it showed a decreasing trend from road runoff to drainage runoff (mean, 3.01 mg/L), with the highest PON concentration in road runoff. The reason for this difference is primarily attributed to the large vegetated area consisting of trees and grasses at BNU which can trap a relatively larger amount of particulate matter present in road runoff.

The NO_3^--N concentration in the roof runoff from BNU (mean, 2.21 mg/L) was slightly less than that from FSC (mean, 2.65 mg/L). The NO_3^--N concentration in road runoff from BNU (mean: 0.90 mg/L) was significantly lower than that from FSC (mean, 1.90 mg/L; ANOVA, $p < 0.05$). The NO_3^--N concentration in drainage flow from BNU (mean, 0.40 mg/L) was significantly lower than at FSC (mean, 2.24 mg/L; ANOVA, $p < 0.05$). This indicates that the NO_3^--N concentration in stormwater from BNU was significantly lower than in FSC during stormwater transport, which is attributed to the fact that BNU features relatively larger aggregated permeable surfaces, which can enhance the prevention of NO_3^--N production (Shen et al., 2015). In addition, the complex boundary of permeable surfaces at BNU promotes interaction with runoff from impermeable surfaces. Therefore, it contributes positively to the storage and retention of NO_3^--N.

Consequently, the landscape pattern is crucial for regulating NO_3^--N concentration in urban stormwater runoff and an optimal spatial arrangement of permeable/impermeable patches can play a key role in reducing NO_3^--N concentration. In conclusion, a large aggregated permeable area with a complex shape can contribute to lowering NO_3^--N and PON concentrations in urban stormwater runoff.

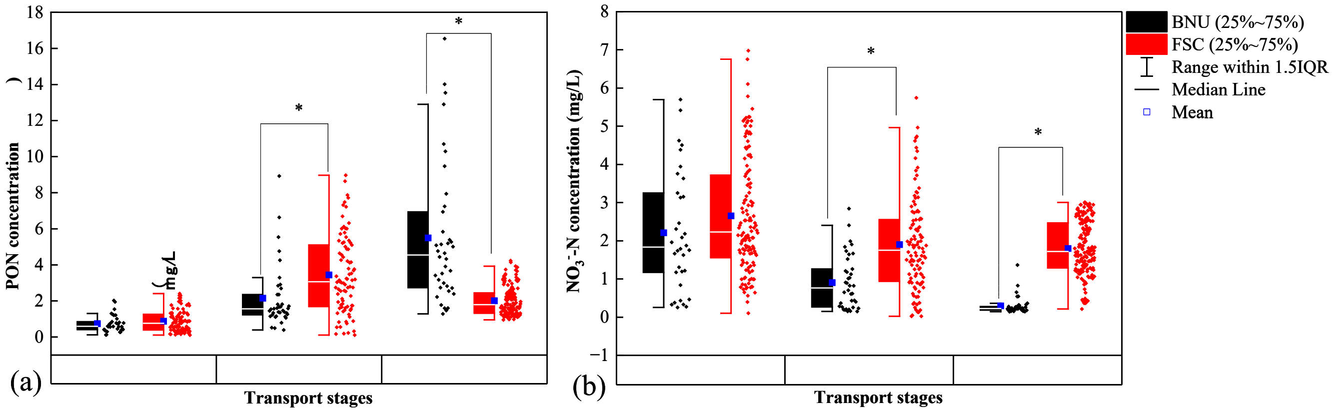

Figure 2. Concentrations of NO_3^--N and PON in stormwater runoff samples. (Note: Figure (a) shows the PON concentrations at different transport stages. Figure

(b) shows the concentrations of NO_3^--N at different transport stages. Significant differences (ANOVA, $p < 0.05$) are denoted by *.)

3.3 Differences in source contributions of NO_3^--N and PON to urban stormwater runoff

Figure 3 illustrates the difference in the contribution from each transport stage to NO_3^--N and PON in stormwater runoff from BNU and FSC. The contribution of each transport stage reflects the proportional relationship between the fluxes of the transport stages, where the flux is the product of the pollutant concentration and runoff volume. As shown in Figure 3, no significant difference is evident in the PON contributions from roof runoff and drainage sediments between BNU and FSC, while the contribution from road runoff to PON shows significant differences between the two catchments. In addition, road runoff generally yields more PON compared to the other transportation stages. The PON contribution from road runoff at BNU (mean, 49%) is significantly lower than at FSC (mean, 67%; ANOVA, $p < 0.05$). Further, no significant difference was noted in the NO_3^--N contribution from roof runoff and rainwater between BNU and FSC. However, the NO_3^--N contribution from road runoff from BNU (mean, 28%) was significantly lower than that from FSC (mean, 34%; ANOVA, $p < 0.05$). The difference between the contribution from road runoff to NO_3^--N and PON is attributed to the fact that the road network at BNU is connected to an aggregated permeable surface area, which has a greater retention effect on runoff. Furthermore, the complex and long pathways along the permeable patches at BNU decrease the propagation rate of runoff. Additionally, the higher connectivity of the permeable surfaces at BNU increases the continuity of the runoff retention effect of the green spaces near the roads. Therefore, the road runoff from BNU is retained more effectually than at FSC. Runoff volume is considered a key factor that affects pollutant fluxes in urban stormwater runoff. When the runoff volume decreases, the residence time of the runoff on the catchment surface increases, and the ability of microorganisms to transform nitrogen is strengthened. This may result in a lower contribution to NO_3^--N and PON by road runoff (Huan et al., 2011; Jun et al., 2023; Peng et al., 2019a). In addition, the lower concentration of NO_3^--N and PON in the road runoff from BNU (Figure 2) may also result in its lower contribution to NO_3^--N and PON pollution in stormwater.

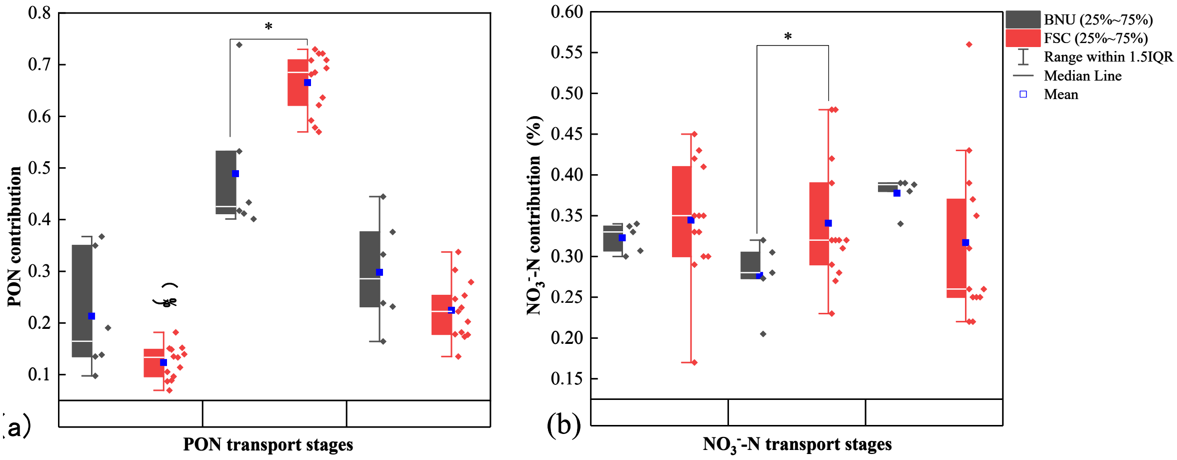

Figure 3. Contributions of different nitrate sources to drainage flow. (Note: Figure (a) shows the contribution of PON at different transport stages. Figure (b) shows the contribution of NO_3^--N at different transport stages. Significant differences (ANOVA, $p < 0.05$) are denoted by *.

4. DISCUSSION

4.1 Effect of landscape pattern on transport and sources of NO_3^--N and PON in stormwater runoff

An appropriate landscape pattern of permeable/impermeable patches significantly affects the transport and sources of NO_3^--N and PON because of the strong ability to retain pollutants on permeable surfaces (Jiang et al., 2020; Ma and Zhao, 2022b). Landscape pattern indices of permeable patches such as woodland and grasslands have been widely used to quantify the effect of landscape patterns on nitrogen pollution generated by urban catchments (Billmire and Koziol, 2018; Li et al., 2015b; Teixeira and Marques, 2016b). However, the effect of permeable/impermeable surface patterns on NO_3^--N and PON concentration during stormwater transport and the source contribution of each transport stage to NO_3^--N and PON has not been adequately investigated to-date. This study contributed to meeting this knowledge gap.

Figure 4 shows the correlation between NO_3^--N and PON concentration at different stormwater transport stages, source contribution, and landscape pattern indices. MPI, LPI, LSI, MSI and CONNECT are negatively correlated with NO_3^--N concentrations in road runoff and drainage flow, as well as with PON concentrations in road runoff, whereas SPLIT shows the opposite with the concentrations of NO_3^--N and PON during the corresponding transport stages. This indicates that less fragmentation (higher MPI and LPI), more complex shapes and profiles (higher LSI and MSI), and higher aggregation (higher CONNECT and lower SPLIT) of permeable patches significantly reduces the NO_3^--N concentrations in road runoff and drainage flow, as well as the PON concentration in road runoff. In addition, MPI, LPI, LSI, MSI, and CONNECT are negatively correlated with the contributions to NO_3^--N and PON by road runoff, whereas SPLIT shows an inverse correlation with the contributions of NO_3^--N and PON by road runoff. This indicates that less fragmentation, more complex shapes and profiles, and higher aggregation of permeable patches significantly reduce the contributions to NO_3^--N and PON by road runoff. The significant reduction of nitrogen pollution in road runoff is attributed to the higher nitrogen retention by larger permeable patches (i.e. less fragmentation), which imposes a greater effect on reducing road runoff volume, reducing NO_3^--N concentrations, and adsorbing and converting PON (Lewis and Grimm, 2007; Zhang et al., 2019b). Consequently, the adjacent permeable patches enhance the exchange of materials and energy, thus facilitating the reduction of NO_3^--N and PON in road runoff. In terms of complexity, the contours and shapes of permeable patches drive pollution sinks. Complex shapes elongate the pollutant transport paths and increase road runoff losses due to permeable surfaces (Yang et al., 2004). In terms of aggregation, higher connectivity between permeable patches enhances their ability to intercept runoff from road surfaces (Meng et al., 2021; Peng et al., 2019b), as well as increases the exchange of materials and energy for promoting the uptake of NO_3^--N and PON, thus enhancing their ecological functions in regulating NO_3^--N and PON concentrations. Therefore, reduced fragmentation, more complex shapes and profiles, and higher aggregation of permeable patches in urban catchments should be considered for mitigating NO_3^--N and PON pollution in stormwater, especially road runoff.

Other than for the reduction of nitrogen pollution in road runoff, the landscape pattern indices were also found to influence the pollution in roof and drainage flow. Figure 4(a) shows that PON concentration in drainage flow has a strong positive correlation with MPI, LPI, LSI, MSI and CONNECT, and a negative correlation with SPLIT. This is because larger and more aggregated patches of lawn and woodland will contain relatively larger amounts of vegetation. Consequently, increased amounts of vegetation debris are generated. These plant residues will enter the drainage system via a rainwater grate and build-up in the drainage pipes. During rainfall, these built-up pollutants can contribute a significant amount of PON to drainage flows. Meanwhile, MPI, LPI, LSI, MSI, and CONNECT show a strong positive correlation to the contribution to PON by roof runoff and drainage sediments (Figure 4(b)). The high contribution to PON by roof runoff is attributed to the lack of stormwater management measures for roofs. Considering the weak correlation between landscape pattern indices and PON concentrations in roof runoff, the volume of roof runoff is the main reason for the high contribution to PON. The large contribution of drainage sediments to PON is due to its increased concentration in drainage flow. Thus, appropriate strategies including LID should be applied to both roofs and drainage networks.

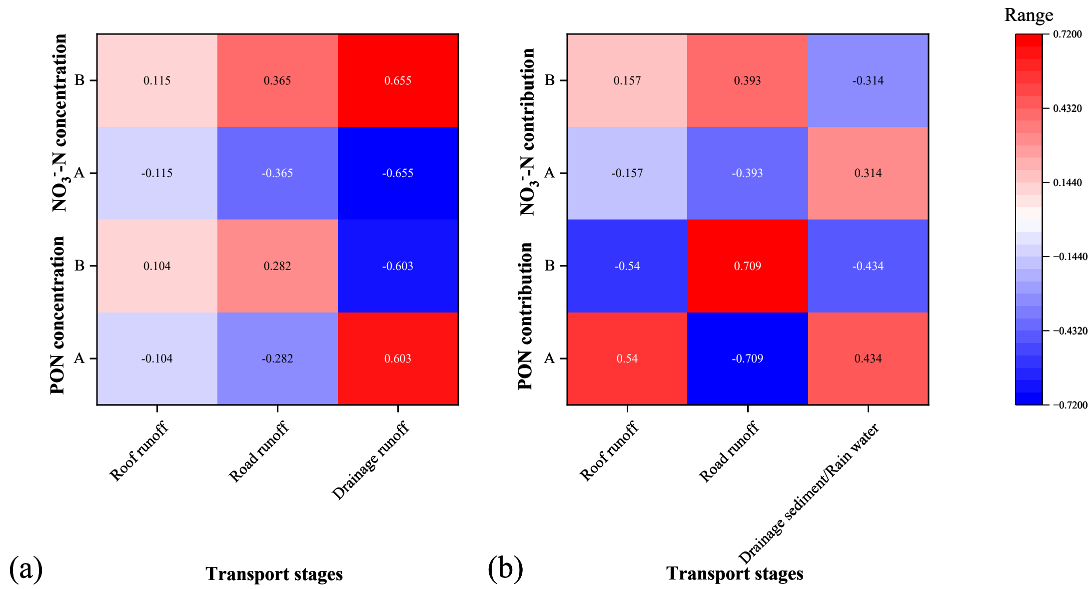

Figure 4. Correlation between NO_3^--N and PON concentration at different stormwater transport stages: source contribution and landscape indices. (Note: (a) shows the heat map of the correlation between the concentrations of NO_3^--N and PON at different transport stages and the landscape pattern index; (b) shows the heat map of the correlation between the contribution of primary sources and the landscape pattern index; A represents landscape pattern indices MPI, LPI, LSI, MSI, and CONNECT; and B represents landscape pattern index SPLIT.)

4.2 Practical application of the research findings

Landscape patterns of permeable/impermeable patches in urban catchments should be considered for the effective application of LID to mitigate stormwater pollution (Jiang et al., 2020; Ma and Zhao, 2022b). LID is becoming increasingly popular for alleviating urban stormwater pollution by inserting permeable surfaces within impermeable surfaces (Jiang et al., 2020; Liu et al., 2021). Examples of LID include green roofs, bioretention ponds and artificial wetlands, which can play an important role in mitigating the increase in runoff volume and stormwater pollutants resulting from impermeable surfaces (Kong et al., 2021; Liu et al., 2021). The combination of local LID master plans and regional landscape planning is ideal for controlling urban stormwater pollution (Li et al., 2018; Zhang et al., 2017). Based on the relationship between transport and sources of NO_3^--N and PON in urban catchments and landscape patterns, recommendations are provided to mitigate urban stormwater nitrogen pollution by the appropriate spatial arrangement of LID in urban catchments.

This study found that lower fragmentation, higher complexity and greater aggregation of permeable patches are effective in reducing NO_3^--N and PON pollution. Accordingly, a few larger areas of permeable patches are preferable over multiple small areas of permeable patches. The former type of landscape pattern is essential for reducing NO_3^-

-N and PON contributions by road runoff. The use of permeable areas such as lawns to connect LIDs can also be considered to reduce their dispersion and increase the connectivity between LIDs and the individual permeable areas to facilitate retention of NO_3^--N, PON and runoff volume. In addition, LID designed with complex boundaries and connected LID groups are favored to reduce NO_3^--N and PON in stormwater runoff. For example, rain gardens and grass swales on roads are effective natural purification and bioretention techniques for stormwater management. Connecting them in series to increase runoff pathways and complexity can simultaneously decrease cumulative runoff and pollutant loads (Davis et al., 2012; Sharma and Malaviya, 2021; Wang et al., 2014). It is also recommended that LID technologies such as green roofs (Alim et al., 2023) should be adopted to minimize the roof runoff volume. It is noted that LID technologies for roof runoff can be applied to newly developing areas, and in the case of developed urban areas, other measures should be considered. Further, the appropriate selection of plants for green roofs can also be incorporated into the green infrastructure to improve its effectiveness in stormwater runoff treatment (Farrell et al., 2022). Further, drainage desilting before the rainy season is also recommended to minimize the nitrogen load in drainage flow during rainfall events. It is important to note that this study primarily investigated the influence of landscape patterns of permeable surfaces on roof and road runoff. Therefore, landscape patterns of permeable patches with lower fragmentation, more complex contours, and higher aggregation could more effectively reduce nitrogen pollution from roof runoff and road runoff. However, there are still limitations in the reduction of runoff pollution in drainage systems. For example, it was found that PON concentration in drainage runoff was higher with these landscape patterns, and thus further measures should be conducted to remove drainage sediments.

5. Conclusions

In this study, the influence of the landscape pattern of permeable/impermeable patches in urban catchments on the transport and sources of NO_3^--N and PON in stormwater runoff were investigated. Six landscape pattern indices (MPI, LPI, MSI, LSI, CONNECT, and SPLIT) were selected to describe the effects of fragmentation, complexity and connectivity on the concentrations and source contributions of NO_3^--N and PON in urban stormwater runoff. The study outcomes confirmed that relatively large permeable patches, complex shape, and good connectivity can significantly reduce the NO_3^--N concentrations in road runoff and drainage flow and PON concentrations in road runoff. Further, the above landscape pattern is effective for mitigating the contributions of NO_3^--N and PON from road runoff. Therefore, LID measures can be installed in urban catchments linking with permeable patches such as lawns to reduce fragmentation and to increase the connectivity of permeable areas. Furthermore, LIDs designed with complex boundaries are favored to increase the effectiveness of permeable patches.

Acknowledgement

This research was supported by the National Natural Science Foundation of China (No. 42077377) and the Fundamental Research Funds for the Central Universities (No. 2019NTST09).

References

Alim, M.A., Jahan, S., Rahman, A., Rahman, M.A., Liebman, M., Garner, B., Griffith, R., Griffith, M., Tao, Z., 2023. Experimental investigation of a multilayer detention roof for stormwater management. J Clean Prod 395 (136413). https://coi.org/10.1016/j.jclepro.2023.136413.

Balasuriya, B.T.G., Ghose, A., Gheewala, S.H., Prapaspongsa, T., 2022. Assessment of eutrophication potential from fertiliser application in agricultural systems in thailand. Sci Total Environ 833 (154993). https://coi.org/10.1016/j.scitotenv.2022.154993.

Billmire, M., Koziol, B.W., 2018. Landscape and flow path-based nutrient loading metrics for evaluation of in-stream water quality in saginaw bay, michigan. J Great Lakes Res 44 (5), 1068-1080. https://coi.org/10.1016/j.jglr.2018.06.004.

Brown, R.A., Borst, M., 2015. Nutrient infiltrate concentrations from three permeable pavement types. J Environ Manage 164, 74-85. https://coi.org/10.1016/j.jenvman.2015.08.038.

Chen, D., Guo, Z., 2022. The source, transport, and removal of chemical elements in rainwater in china. Sustainability 14 (1243919). https://coi.org/10.3390/su141912439.

Christensen, A.A., Andersen, P.S., Piil, K., Andersen, E., Vejre, H., Graversgaard, M., 2019. Pursuing implementation solutions for targeted nitrogen management in agriculture- a novel approach to synthesize knowledge and facilitate sustainable decision making based on collaborative landscape modelling. J Environ Manage 246, 679-686. https://coi.org/10.1016/j.jenvman.2019.05.107.

Christensen, B.T., Pedersen, B.F., Olesen, J.E., Eriksen, J., 2021. Land-use and agriculture in denmark around year 1900 and the quest for eu water framework directive reference conditions in coastal waters. Ambio 50 (10), 1882-1893. https://coi.org/10.1007/s13280-021-01536-8.

Davis, A.P., Stagge, J.H., Jamil, E., Kim, H., 2012. Hydraulic performance of grass swales for managing highway runoff. Water Res 46 (20SI), 6775-6786. https://coi.org/10.1016/j.watres.2011.10.017.

Deletic, A., 1998. The first flush load of urban surface runoff. Water research (Oxford) 32 (8), 2462-2470. https://coi.org/10.1016/S0043-1354(97)00470-3.

Ding, X., Shi, J., Guo, X., Gao, H., Liu, S., Guo, W., 2023. Interannual variations in the nutrient cycle in the central bohai sea in response to anthropogenic inputs. Chemosphere 313 (137620). https://coi.org/10.1016/j.chemosphere.2022.137620.

Duan, B., Zhao, J., Gao, Y., Zhu, D., Hua, Y., Zhou, W., 2013. Control effect of green roofs on roof runoff pollutants. Environmental Science & Technology (China) 36 (9), 57-117.

Eckart, K., Mcphee, Z., Bolisetti, T., 2017. Performance and implementation of low impact development - a review. Sci Total Environ 607, 413-432. https://coi.org/10.1016/j.scitotenv.2017.06.254.

Farrell, C., Livesley, S.J., Arndt, S.K., Beaumont, L., Burley, H., Ellsworth, D., Esperon-Rodriguez, M., Fletcher, T.D., Gallagher, R., Ossola, A., Power, S.A., Marchin, R., Rayner, J.P., Rymer, P.D., Staas, L., Szota, C., Williams, N.S.G., Leishman, M., 2022. Can we integrate ecological approaches to improve plant selection for green infrastructure? Urban for Urban Green 76 (127732). https://coi.org/10.1016/j.ufug.2022.127732.

Ferreira, C.S.S., Walsh, R.P.D., de Lourdes Costa, M., Coelho, C.O.A., Ferreira, A.J.D., 2016. Dynamics of surface water quality driven by distinct urbanization patterns and storms in a portuguese peri-urban catchment. J Soils Sediments 16 (11), 2606-2621. https://coi.org/10.1007/s11368-016-1423-4.

Hu, M., Yao, M., Wang, Y., Pan, Z., Wu, K., Jiao, X., Chen, D., 2023. Influence of nitrogen inputs, dam construction and landscape patterns on riverine nitrogen exports in the yangtze river basin during 1980-2015. J Hydrol (Amst) 617 (129109C). https://coi.org/10.1016/j.jhydrol.2023.129109.

Huan, W., Kun, L., Zi-Cheng, L.I., Zheng, Z., Li, Z., 2011. Analysis of major pollutants flux into the sea and influencing factors on the north shore of the liaodong gulf. Hai Yang Xue Bao 33 (6), 110-116.

Huang, C., Lao, Q., Chen, F., Zhang, S., Chen, C., Bian, P., Zhu, Q., 2021. Distribution and sources of particulate organic matter in the northern south china sea: implications of human activity. J Ocean Univ China 20 (5), 1136-1146. https://coi.org/10.1007/s11802-021-4807-z.

Jani, J., Yang, Y., Lusk, M.G., Toor, G.S., 2020. Composition of nitrogen in urban residential stormwater runoff: concentrations, loads, and source characterization of nitrate and organic nitrogen. Plos One 15 (2), e229715. https://coi.org/10.1371/journal.pone.0229715.

Jiang, C., Li, J., Li, H., Li, Y., Zhang, Z., 2020. Low-impact development facilities for stormwater runoff treatment: field monitoring and assessment in xi’an area, china. J Hydrol (Amst) 585, 124803. https://coi.org/10.1016/j.jhydrol.2020.124803.

Jiang, Z., Liao, Y., Xie, W., Li, J., Fang, Z., Zhao, H., Li, X., 2020. [influence of pervious/impervious pattern on runoff and pollution in parcel-based catchment]. Huan jing ke xue= Huanjing kexue 41 (10). https://coi.org/10.13227/j.hjkx.202003221.

Jiang, Z., Liao, Y., Xie, W., Li, J., Fang, Z.D., Zhao, H.T., Li, X.Y., 2020. Influence of pervious/impervious pattern on runoff and pollution in parcel-based catchment. Huan Jing ke Xue= Huanjing Kexue 41 (10), 4599-4606.

Jun, W., Jieyu, H., Fangyuan, L.I., Xiaoyan, W., 2023. Influence of anthropogenic nitrogen input on river nitrate nitrogen flux in the chaohe river watershed. Journal of Agro-Environment Science 42 (1), 142-154. https://coi.org/10.11654/jaes.2022-0315.

Kamali, M., Delkash, M., Tajrishy, M., 2017. Evaluation of permeable pavement responses to urban surface runoff. J Environ Manage 187, 43-53. https://coi.org/10.1016/j.jenvman.2016.11.027.

Kong, Z., Shao, Z., Shen, Y., Zhang, X., Chen, M., Yuan, Y., Li, G., Wei, Y., Hu, X., Huang, Y., He, Q., Chai, H., 2021. Comprehensive evaluation of stormwater pollutants characteristics, purification process and environmental impact after low impact development practices. J Clean Prod 278 (123509). https://coi.org/10.1016/j.jclepro.2020.123509.

Lewis, D.B., Grimm, N.B., 2007. Hierarchical regulation of nitrogen export from urban catchments: interactions of storms and landscapes. Ecol Appl 17 (8), 2347-2364. https://coi.org/10.1890/06-0031.1.

Li, S., Xiu, D.X., Shi, T.M., Zhou, S.W., Fu, S.L., Yu, C., 2018. Landscape ecological planning of coastal industrial park based on low impact development concept: a case of the second coastal industrial base in yingkou city, liaoning province, china. Ying yong sheng tai xue bao = The journal of applied ecology 29 (10). https://coi.org/10.13287/j.1001-9332.201810.009.

Li, Y., Li, Y., Qureshi, S., Kappas, M., Hubacek, K., 2015a. On the relationship between landscape ecological patterns and water quality across gradient zones of rapid urbanization in coastal china. Ecol Modell 318, 100-108. https://coi.org/10.1016/j.ecolmodel.2015.01.028.

Li, Y., Li, Y., Qureshi, S., Kappas, M., Hubacek, K., 2015b. On the relationship between landscape ecological patterns and water quality across gradient zones of rapid urbanization in coastal china. Ecol Modell 318, 100-108. https://coi.org/10.1016/j.ecolmodel.2015.01.028.

Liu, T., Lawluvy, Y., Shi, Y., Yap, P., 2021. Low impact development (lid) practices: a review on recent developments, challenges and prospects. Water Air Soil Pollut 232 (3449). https://coi.org/10.1007/s11270-021-05262-5.

Lucke, T., Drapper, D., Hornbuckle, A., 2018. Urban stormwater characterisation and nitrogen composition from lot-scale catchments — new management implications. Sci Total Environ 619-620, 65-71. https://coi.org/10.1016/j.scitotenv.2017.11.105.

Lusk, M.G., Toor, G.S., Inglett, P.W., 2020. Organic nitrogen in residential stormwater runoff: implications for stormwater management in urban watersheds. Sci Total Environ 707, 135962. https://coi.org/10.1016/j.scitotenv.2019.135962.

Ma, Y., Wang, S., Zhang, X., Shen, Z., 2021. Transport process and source contribution of nitrogen in stormwater runoff from urban catchments. Environ Pollut 289, 117824. https://coi.org/10.1016/j.envpol.2021.117824.

Ma, Y., Zhao, H., 2022a. The role of spatial patterns of low impact development in urban runoff pollution control within parcel based catchments. Front Environ Sci 10 (926937). https://coi.org/10.3389/fenvs.2022.926937.

Ma, Y., Zhao, H., 2022b. The role of spatial patterns of low impact development in urban runoff pollution control within parcel based catchments. Front Environ Sci 10. https://coi.org/10.3389/fenvs.2022.926937.

Mcaleer, E., Coxon, C., Mellander, P., Grant, J., Richards, K., 2022. Patterns and drivers of groundwater and stream nitrate concentrations in intensively managed agricultural catchments. Water (Basel) 14 (13889). https://coi.org/10.3390/w14091388.

Mcilvin, M.R., Casciotti, K.L., 2011. Technical updates to the bacterial method for nitrate isotopic analyses. Anal Chem 83 (5), 1850-1856. https://coi.org/10.1021/ac1028984.

Meng, C., Liu, H., Li, Y., Wang, Y., Li, X., Shen, J., Fan, X., Li, Y., Wu, J., 2021. Influences of the landscape pattern on riverine nitrogen exports derived from legacy sources in subtropical agricultural catchments. Biogeochemistry 152, 161-177.

Meng, D., Cheng, H., Shao, Y., Luo, M., Xu, D., Liu, Z., Ma, L., 2022. Progress on the effect of nitrogen on transformation of soil organic carbon. Processes (Basel) 10 (242511). https://coi.org/10.3390/pr10112425.

Pamuru, S.T., Forgione, E., Croft, K., Kjellerup, B.V., Davis, A.P., 2022. Chemical characterization of urban stormwater: traditional and emerging contaminants. Sci Total Environ 813 (151887).

https://coi.org/10.1016/j.scitotenv.2021.151887.

Parnell, A.C., Phillips, D.L., Bearhop, S., Semmens, B.X., Ward, E.J., Moore, J.W., Jackson, A.L., Grey, J., Kelly, D.J., Inger, R., 2013. Bayesian stable isotope mixing models. Environmetrics 24 (6), 387-399. https://coi.org/10.1002/env.2221.

Peng, H., Liu, Y., Wang, H., Gao, X., Ma, L., 2016. Event mean concentration and first flush effect from different drainage systems and functional areas during storms. Environ Sci Pollut Res Int 23 (6), 5390-5398. https://coi.org/10.1007/s11356-015-5657-2.

Peng, Q., Li, Z., Deng, X., Su, M., 2019a. Nitrogen and phosphorus deposition in urban lakes and its impact factors: a case study of east lake in wuhan. Acta Sci. Circumstantiae 39, 2635-2643.

Peng, Q., Li, Z., Deng, X., Su, M., 2019b. Nitrogen and phosphorus deposition in urban lakes and its impact factors: a case study of east lake in wuhan. Acta Sci. Circumstantiae 39, 2635-2643.

Perera, T., Mcgree, J., Egodawatta, P., Jinadasa, K.B.S.N., Goonetilleke, A., 2021. Catchment based estimation of pollutant event mean concentration (emc) and implications for first flush assessment. J Environ Manage 279 (111737). https://coi.org/10.1016/j.jenvman.2020.111737.

Peter, K.T., Lundin, J.I., Wu, C., Feist, B.E., Tian, Z., Cameron, J.R., Scholz, N.L., Kolodziej, E.P., 2022. Characterizing the chemical profile of biological decline in stormwater-impacted urban watersheds. Environ Sci Technol 56 (5), 3159-3169. https://coi.org/10.1021/acs.est.1c08274.

Pilon, C., Moore, P.A., Pote, D.H., Martin, J.W., Owens, P.R., Ashworth, A.J., Miller, D.M., Delaune, P.B., 2019. Grazing management and buffer strip impact on nitrogen runoff from pastures fertilized with poultry litter. J Environ Qual 48 (2), 297-304. https://coi.org/10.2134/jeq2018.04.0159.

Pour, S.H., Abd Wahab, A.K., Shahid, S., Asaduzzaman, M., Dewan, A., 2020. Low impact development techniques to mitigate the impacts of climate-change-induced urban floods: current trends, issues and challenges. Sustain Cities Soc 62 (102373). https://coi.org/10.1016/j.scs.2020.102373.

Priestley, S.C.C., Tyler, J., Liebelt, S.R.R., Mosley, L.M.M., Wong, W.W., Shao, Y., Woolston, Z., Farrell, M., Welsh, D.T.T., Brookes, J.D.D., Collins, A.S.S., Keneally, C., Farkas, J., 2022. N and c isotope variations along an extreme eutrophication and salinity gradient in the coorong lagoon, south australia. Front Earth Sci (Lausanne) 9 (727971). https://coi.org/10.3389/feart.2021.727971.

Sharma, R., Malaviya, P., 2021. Management of stormwater pollution using green infrastructure: the role of rain gardens. Wires Water 8 (e15072). https://coi.org/10.1002/wat2.1507.

Shen, Z., Hou, X., Li, W., Aini, G., 2014. Relating landscape characteristics to non-point source pollution in a typical urbanized watershed in the municipality of beijing. Landsc Urban Plan 123, 96-107. https://coi.org/10.1016/j.landurbplan.2013.12.007.

Shen, Z., Hou, X., Li, W., Aini, G., Chen, L., Gong, Y., 2015. Impact of landscape pattern at multiple spatial scales on water quality: a case study in a typical urbanised watershed in china. Ecol Indic 48, 417-427. https://coi.org/10.1016/j.ecolind.2014.08.019.

Simpson, I.M., Winston, R.J., Brooker, M.R., 2022. Effects of land use, climate, and imperviousness on urban stormwater quality: a meta-analysis. Sci Total Environ 809, 152206. https://coi.org/10.1016/j.scitotenv.2021.152206.

Teixeira, Z., Marques, J.C., 2016a. Relating landscape to stream nitrate-n levels in a coastal eastern-atlantic watershed (portugal). Ecol Indic 61, 693-706. https://coi.org/10.1016/j.ecolind.2015.10.021.

Teixeira, Z., Marques, J.C., 2016b. Relating landscape to stream nitrate-n levels in a coastal eastern-atlantic watershed (portugal). Ecol Indic 61, 693-706. https://coi.org/10.1016/j.ecolind.2015.10.021.

Wang, J., Li, T., Hou, J., Chen, Y., 2014. Coliforms in road runoff and its removal by rain gardens. Chinese Journal of Environmental Engineering 8 (1673-9108(2014)8:12<5221:LMJLDD>2.0.TX;2-Y12), 5221-5225.

Wang, S., Ma, Y., Zhang, X., Shen, Z., 2022. Transport and sources of nitrogen in stormwater runoff at the urban catchment scale. Sci Total Environ 806, 150281. https://coi.org/10.1016/j.scitotenv.2021.150281.

Wu, J.S., Allan, C.J., Saunders, W.L., Evett, J.B., 1998. Characterization and pollutant loading estimation for highway runoff. J Environ Eng (New York) 124 (7), 584-592.

Wu, S., Tetzlaff, D., Yang, X., Soulsby, C., 2022. Disentangling the influence of landscape characteristics, hydroclimatic variability and land management on surface water no3-n dynamics: spatially distributed modeling over 30 yr in a lowland mixed land use catchment. Water Resour Res 58 (e2021WR0305662). https://coi.org/10.1029/2021WR030566.

Wu, W., Wang, Y., Liu, M., Li, C., 2021. A review on the use of landscape indices to study the effects of three-dimensional urban landscape patterns on haze pollution in china. Pol J Environ Stud 30 (4), 2957-2967. https://coi.org/10.15244/pjoes/130900.

Xie, H., Huang, C., Li, J., Zhang, Y., Xu, X., Liu, D., Ouyang, Z., 2021. Strong precipitation and human activity spur rapid nitrate deposition in estuarine delta: multi-isotope and auxiliary data evidence. INTERNATIONAL JOURNAL OF ENVIRONMENTAL RESEARCH AND PUBLIC HEALTH 18 (622112). https://coi.org/10.3390/ijerph18126221.

Xu, T., Li, K., Engel, B.A., Jia, H., Leng, L., Sun, Z., Yu, S.L., 2019. Optimal adaptation pathway for sustainable low impact development planning under deep uncertainty of climate change: a greedy strategy. J Environ Manage 248 (109280). https://coi.org/10.1016/j.jenvman.2019.109280.

Yang, L., Ma, K., Guo, Q., Zhao, J., 2004. [impacts of the urbanization on waters non-point source pollution]. Huan jing ke xue= Huanjing kexue 25 (6).

Zhang, J., Wang, J., Xiu, D., Li, S., 2017. Control and landscape design planning method of runoff in east liaoyang based on lid. Journal of Shenyang Jianzhu University. Natural Science 33 (2095-1922(2017)33:2<363:JYLDDL>2.0.TX;2-B2), 363-370.

Zhang, L., Lu, W., Hou, G., Gao, H., Liu, H., Zheng, Y., 2019a. Coupled analysis on land use, landscape pattern and nonpoint source pollution loads in shitoukoumen reservoir watershed, china. Sustain Cities Soc 51, 101788. https://coi.org/10.1016/j.scs.2019.101788.

Zhang, L., Lu, W., Hou, G., Gao, H., Liu, H., Zheng, Y., 2019b. Coupled analysis on land use, landscape pattern and nonpoint source pollution loads in shitoukoumen reservoir watershed, china. Sustain Cities Soc 51, 101788. https://coi.org/10.1016/j.scs.2019.101788.

Zhang, Y., Smith, J.A., Luo, L., Wang, Z., Baeck, M.L., 2014. Urbanization and rainfall variability in the beijing metropolitan region. J Hydrometeorol 15 (6), 2219-2235. https://coi.org/10.1175/JHM-D-13-0180.1.